

# EnzyPGM: Pocket-conditioned Generative Model for Substrate-specific Enzyme Design

Zefeng Lin<sup>1</sup>, Zhihang Zhang<sup>4</sup>, Weirong Zhu<sup>1</sup>, Tongchang Han<sup>1</sup>

Xianyong Fang<sup>3\*</sup>, Tianfan Fu<sup>2†</sup>, Xiaohua Xu<sup>1‡</sup>

<sup>1</sup>School of Computer Science and Technology, University of Science and Technology of China, Hefei, Anhui, China

<sup>2</sup>State Key Laboratory for Novel Software Technology at Nanjing University, School of Computer Science, Nanjing University, Nanjing, Jiangsu, China

<sup>3</sup>School of Computer Science and Technology, Anhui University, Hefei, Anhui, China

<sup>4</sup>School of Airspace Science and Engineering, Shandong University, Jinan, Shandong, China

{zflin, zwr211355, tchan, xiaohuaxu}@mail.ustc.edu.cn, futianfan@nju.edu.cn, fangxianyong@ahu.edu.cn, 202200800170@mail.sdu.edu.cn

## Abstract

Designing enzymes with substrate-binding pockets is a critical challenge in protein engineering, as catalytic activity depends on the precise interaction between pockets and substrates. Currently, generative models dominate functional protein design but cannot model pocket-substrate interactions, which limits the generation of enzymes with precise catalytic environments. To address this issue, we propose **EnzyPGM**, a unified framework that jointly generates enzymes and substrate-binding pockets conditioned on functional priors and substrates, with a particular focus on learning accurate pocket-substrate interactions. At its core, **EnzyPGM** includes two main modules: a Residue-atom Bi-scale Attention (RBA) that jointly models intra-residue dependencies and fine-grained interactions between pocket residues and substrate atoms, and a Residue Function Fusion (RFF) that incorporates enzyme function priors into residue representations. Also, we curate EnzyPock, an enzyme-pocket dataset comprising 83,062 enzyme-substrate pairs across 1,036 four-level enzyme families. Extensive experiments demonstrate that **EnzyPGM** achieves state-of-the-art performance on EnzyPock. Notably, **EnzyPGM** reduces the average binding energy of 0.47 kcal/mol over EnzyGen, showing its superior performance on substrate-specific enzyme design. The code and dataset will be released later.

## 1 Introduction

Enzymes are nature’s most efficient biocatalysts, accelerating chemical reactions by  $10^3$ – $10^{17}$  fold [Bar-Even *et al.*,

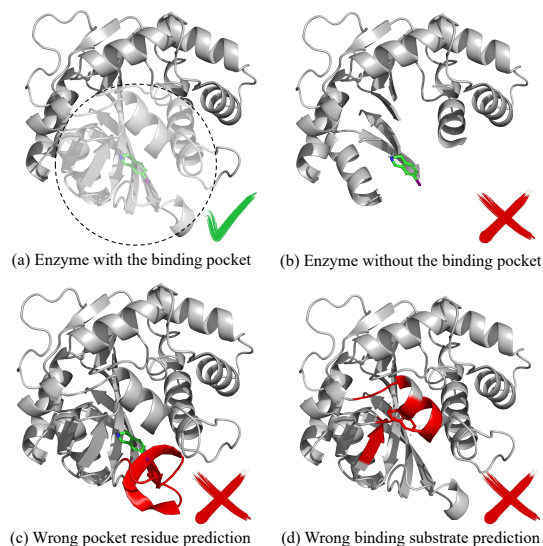


Figure 1: Four cases of enzyme design. None of the enzymes in (b), (c), and (d) bind to the substrate because there are no pockets in (b), and atom clashes in (c) and (d), which are represented by red.

2011] while maintaining unique substrate specificity [Huang *et al.*, 2021]. The catalytic activity of enzymes arises from precisely folded 3D structures that form confined spatial regions, called substrate-binding pockets [Stank *et al.*, 2016], where specific substrates are recognized, bound, and rapidly transformed into products. Recently, deep learning methods have demonstrated impressive potential for functional protein design [Chu *et al.*, 2024; Kortemme, 2024; Notin *et al.*, 2024], where these methods can be classified as: (1) general functional protein design guided by functional labels and partial protein information [Baek *et al.*, 2021; Nijkamp *et al.*, 2023]; (2) ligand-binding protein design relies on the geometric structure of protein-ligand complexes [Watson *et al.*, 2023; Dauparas *et al.*, 2025]; and (3) substrate-

\*Corresponding author, Email: fangxianyong@ahu.edu.cn

†Corresponding author, Email: futianfan@nju.edu.cn

‡Corresponding author, Email: xiaohuaxu@ustc.edu.cn

specific enzyme design based on the substrate properties and enzyme function [Du *et al.*, 2025; Wang *et al.*, 2025].

**Challenges.** However, joint modeling of enzymes and substrate-binding pockets remains rarely studied as it faces several key challenges: (1) How to learn an effective representation of substrate-binding pockets to capture pocket-substrate interactions? These interactions affect the binding configuration and geometric structure of the enzyme and substrate [Stärk *et al.*, 2022]. Figure 1(b) shows the case without the pocket-substrate interaction modeling, where the predicted enzyme does not have a binding pocket and cannot bind to the substrate. (2) How to accurately model the residues and substrate in the pocket? The minor prediction deviations on residue and substrate significantly reduce catalytic efficiency [Lesk, 2001]. Figure 1(c) and (d) show the cases without accurately modeling the residue and substrate, where the predicted pocket and substrate have an atom clash. (3) A lack of public datasets that contain enzyme and substrate binding pockets.

**Solution.** To tackle these challenges, in this paper, we propose the **Pocket-conditioned Enzyme Generative Model (EnzyPGM)**, which explicitly models the substrate-binding pocket to design substrate-specific enzymes. Our key motivation is to model pocket-substrate interactions by bi-scale representation learning, thereby dynamically adjusting pocket sites in the enzyme to form a valid pocket. Furthermore, given that enzymes have obvious functional categories and functionally conserved sites, we integrate them into the language model for enzyme design. Specifically, we propose the Residue-atom Bi-scale Attention (RBA) module to accurately model the interaction between pocket residues and substrate atoms. It mainly consists of intra-residue and residue-atom attention mechanisms, which individually capture neighborhood correlations among residues, and the interaction between pocket residues and substrate atoms, thus facilitating bi-scale representation learning across pockets and substrates. To fuse the enzyme function and the structure of residues into the residue representation, we employ the Residue Function Fusion (RFF) module. It integrates Enzyme Commission (EC) number as the function embedding and updates residue representations and 3D coordinates based on their spatial neighborhoods. Also, to solve the lack of public datasets in enzyme-pocket modeling, we curate EnzyPock, the first enzyme-pocket dataset comprising 84,336 enzyme-substrate pairs across 1,036 four-level enzyme families and 17,404 PDB entries.

**Main contributions** are summarized as: (1) We propose EnzyPGM, the first model to generate enzyme and substrate-binding pockets conditioned on specific substrates jointly. (2) We design a bi-scale attention mechanism and fuse enzyme function priors, which accurately captures the interaction across residues and substrate atoms to generate a binding pocket. (3) We curate EnzyPock, a refined enzyme-pocket dataset to tackle the lack of datasets for enzyme-pocket jointly modeling. Experimental results show that EnzyPGM consistently outperforms existing methods across on EnzyPock, generating enzymes with higher catalytic activity, structural confidence, and substrate selectivity.

## 2 Related Work

**Deep Learning for Protein Design.** Recent years have witnessed significant progress in protein design driven by deep learning. These protein design methods can be categorized into three paradigms: structure-based inverse folding, *de novo* sequence generation, and joint sequence-structure design. Inverse folding (IF) models aim to obtain amino acid sequences that fold into a given 3D structure. Representative methods, such as ProteinMPNN [Dauparas *et al.*, 2022] and ESM-IF [Hsu *et al.*, 2022], achieve high natural sequence recovery but rely on a given protein backbone. *De novo* sequence generation methods aim at designing novel sequences from scratch. They generate valid sequences by learning evolutionary patterns from large datasets, e.g., ProtGPT2 [Ferruz *et al.*, 2022], DPLM [Wang *et al.*, 2024], and DiMA [Meshchaninov *et al.*, 2025]. Sequence-structure co-design methods generate both sequence and structure jointly based on multi-modal priors, such as equivariant graph neural network (EGNN) [Satorras *et al.*, 2021] and ESM3 [Hayes *et al.*, 2025]. Although these approaches demonstrate strong potential for protein engineering, they fail to consider catalytic functions and substrate-specific requirements, which are critical to enzyme design.

**Ligand-binding Pocket Generation.** Owing to the importance of the ligand-pocket binding in drug design, several studies propose ligand-aware pocket generation frameworks. PocketGen [Zhang *et al.*, 2024a] and PocketFlow [Zhang *et al.*, 2024b] explore protein pocket generation by integrating molecular priors to generate ligand-binding pockets. Despite these advances, most pocket generation models rarely consider the functional prior of proteins and require protein backbones as the generation condition. This limits these approaches to accurately capture protein-substrate interactions and apply to substrate-specific enzyme design.

**Substrate-specific Enzyme Generation.** EnzyGen [Song *et al.*, 2024] formulated enzyme generation as the joint modeling of enzyme sequences and backbones, conditioned on functional residues and substrates. GENzyme [Hua *et al.*, 2024] is a *de novo* design approach that generates pockets, enzymes and substrate-binding complexes in stages. EnzyControl [Song *et al.*, 2025] focuses on enzyme backbone generation by functional and substrate-specific control. However, they do not explicitly model the pocket-substrate interactions, which makes them unable to generate enzymes with high substrate affinity. In contrast, the proposed EnzyPGM integrates substrate-binding pocket modeling directly into the enzyme design, thereby generating practical substrate-specific enzymes.

## 3 EnzyPGM: Pocket-conditioned Enzyme Generative Model

### 3.1 Substrate-specific Enzyme Design

This work aims to design substrate-specific enzymes with the binding pocket by modeling pocket-substrate interactions and fusing enzyme function priors.

An  $N$ -residue enzyme  $\mathcal{E}$  is represented as a sequence of residues  $\mathcal{E} = \{r_1, r_2, \dots, r_N\}$ , where each residue  $r_i = (s_i, x_i)$ , with  $s_i \in \mathcal{A}$  denoting the amino acid type, and  $x_i \in \mathbb{R}^3$  being its 3D coordinate of the  $C_\alpha$  atom. Here,  $\mathcal{A}$

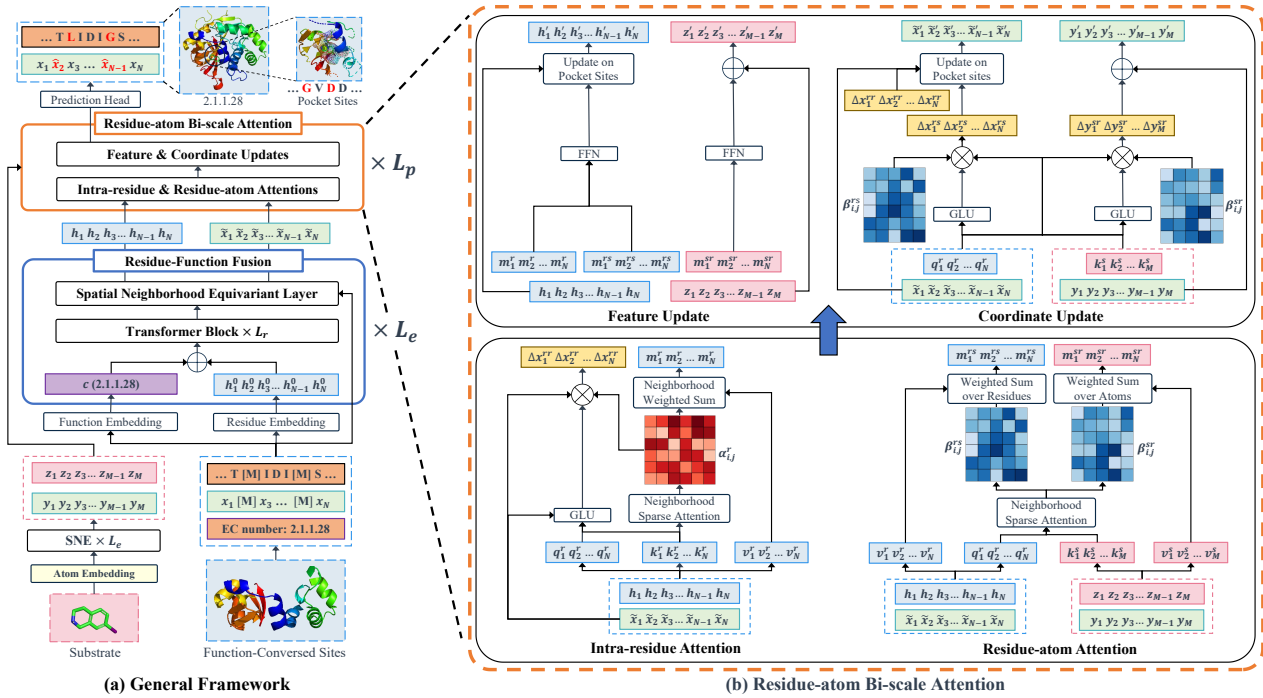


Figure 2: Overview of EnzyPGM. (a) EnzyPGM takes enzyme function-converted sites as a masked input sequence, conditioned on EC number and substrate atom, and predicts the complete enzyme and pocket sites via RFF and RBA modules. The mask sites at the input are represented by [M] both in sequence and coordinate space, their prediction results are indicated in **red** at the output. (b) present the specific process of the intra-residue and residue-atom attention, the feature and coordinate updates.

represents the 20-amino-acid alphabet. A substrate molecule  $\mathcal{V}$  consisting of  $M$  atoms is denoted as  $\mathcal{V} = \{v_1, v_2, \dots, v_M\}$ , where each atom  $v_j = (a_j, y_j)$ , with  $a_j \in \mathbb{R}^5$  representing the five atom-level chemical feature composed of element type, aromaticity, connectivity, hydrogen atom number, and hybridization type, and  $y_j \in \mathbb{R}^3$  being its 3D coordinate.

Given an enzyme  $\mathcal{E}$  and substrate  $\mathcal{V}$ , the substrate-binding pocket  $\mathcal{P}$  is the residue set spatially proximal to the substrate:

$$\mathcal{P} = \{r_i \in \mathcal{E} \mid \min_{v_j \in \mathcal{V}} \|x_i - y_j\|_2 < d\}, \quad (1)$$

where  $\|\cdot\|_2$  denotes the L2 norm, and  $d$  is a distance threshold (in Å) and set to 10 in our practice.

Enzyme Commission (EC) numbers are a standard for enzymes based on catalytic reaction types, where the fourth-level classification precisely defines functional families and provides a basis for inferring enzyme functions via homology [Tipton and Boyce, 2000]. Functionally conserved sites of enzymes are highly conserved across evolution, as these residues directly determine catalytic activity and structural stability, serving as key signatures of enzymes' functions and structures [Capra and Singh, 2007]. To fully utilize these functional priors, we obtain conserved sites  $\mathcal{M}$  under EC label  $c$  as part of the input using multiple sequence alignment (MSA), and then predict other masked sites using a model.

In summary, our study problem can be formulated as a conditional masked language modeling (MLM) task: given a EC label  $c$ , a given substrate  $\mathcal{V}$ , a functionally conserved site index set  $\mathcal{M}$ , its residues set  $\mathcal{E}_{\mathcal{M}}$ , generate a complete

enzyme  $\hat{\mathcal{E}}$  and its substrate-binding pocket  $\hat{\mathcal{P}}$  that can bind the substrate. Essentially, we need to train a generative model to learn the probability  $P(\hat{\mathcal{E}}, \hat{\mathcal{P}} \mid \mathcal{E}_{\mathcal{M}}, \mathcal{V}, c)$ .

## 3.2 Overall Framework

EnzyPGM is proposed for generating enzyme and substrate-binding pockets conditioned on both enzyme functional class and functionally conserved sites (Figure 2 (a)). It mainly consists of two modules: the **Residue Function Fusion (RFF)** and the **Residue-atom Bi-scale Attention (RBA)**.

At a high level, RFF aims to fuse residue-level contextual information from the enzyme sequence with functional priors in EC number and maintain their SE(3)-equivariance, while RBA focuses on enhancing pocket residues in both feature and coordinate spaces selectively.

Next, we will detail the components of EnzyPGM.

## 3.3 Residue-Function Fusion (RFF)

RFF is stacked Transformer [Vaswani *et al.*, 2017] blocks with a function embedding and Spatial Neighborhood Equivariant (SNE) layer. The former embeds the EC number into residue embeddings to obtain function-aware residue embeddings, while the latter performs message passing within the residue neighborhood graphs to ensure SE(3)-equivariance of residue representations and coordinates. We also use the SNE layer to model the substrate atom and coordinates.

Given  $\mathcal{E}$  and  $\mathcal{M}$ , each  $s_i$  in  $\mathcal{E}$  are first embedded into a

residue  $\mathbf{h}_i^{(1)} \in \mathbb{R}^{d_h}$ :

$$\mathbf{h}_i^{(1)} = \begin{cases} \text{Emb}(s_i), & i \in \mathcal{M}, \\ \text{Emb}([\text{mask}]), & \text{otherwise}, \end{cases} \quad (2)$$

where [mask] is the special token to mask the sites we need to predict, and  $d_h$  denotes the dimensions of the representation.

For introducing the enzyme family priors, we encode the EC number  $c$  into a function embedding  $\text{Emb}(c) \in \mathbb{R}^{d_h}$  using a learnable embedding table and add it to the residue embedding. Then, we apply  $L_r$  Transformer blocks with function embedding to model long-range residue dependencies. In the  $t$ -th transformer block, a multi-head self-attention (MHA) and fully connected feedforward network (FFN) are performed to obtain the function-aware residue representation  $\mathbf{h}_i^{(t+1)}$ :

$$\tilde{\mathbf{h}}_i^{(t)} = \mathbf{h}_i^{(t)} + \text{Emb}(c), \quad (3)$$

$$\mathbf{h}_i^{(t+0.5)} = \tilde{\mathbf{h}}_i^{(t)} + \text{MHA}\left(\text{LN}(\tilde{\mathbf{h}}_i^{(t)}), \text{LN}(\tilde{\mathbf{H}}^{(t)})\right), \quad (4)$$

$$\mathbf{h}_i^{(t+1)} = \mathbf{h}_i^{(t+0.5)} + \text{FFN}\left(\text{LN}(\mathbf{h}_i^{(t+0.5)})\right). \quad (5)$$

Here  $\text{LN}(\cdot)$  denotes the layer normalization (LN) operator, Pre-LN instead of Post-LN [Xiong *et al.*, 2020] is adopted, and  $\tilde{\mathbf{H}}^{(t)} = [\tilde{\mathbf{h}}_1^{(t)}, \dots, \tilde{\mathbf{h}}_N^{(t)}]$ .

The output  $\{\mathbf{h}_i^{(L_r+1)}\}_{i=1}^N$  of the last Transformer block and the residue coordinates are then input to the SNE layer to ensure their SE(3)-equivariance:

$$\mathbf{m}_{ik} = \text{FFN}\left(\mathbf{h}_i^{(L_r+1)}; \mathbf{h}_k^{(L_r+1)}; \|x_i - x_k\|_2^2\right), \quad (6)$$

$$\tilde{\mathbf{h}}_i = \text{FFN}\left(\mathbf{h}_i^{(L_r+1)}; \sum_{k \in \mathcal{N}(i)} \mathbf{m}_{ik}\right), \quad (7)$$

$$\tilde{x}_i = x_i + \frac{1}{|\mathcal{N}(i)|} \sum_{k \in \mathcal{N}(i)} (x_i - x_k) \cdot \text{FFN}(\mathbf{m}_{ik}). \quad (8)$$

Here,  $\mathbf{m}_{ik}$  denotes messages exchanged between residues,  $\mathcal{N}(i)$  is the local neighboring nodes set of residue  $r_i$  within a predefined radius,  $|\mathcal{N}(i)|$  represents the number of the set, and  $[\cdot]$  denotes concatenation of vectors. Finally, the SNE layer outputs refined residue representations  $\{\tilde{\mathbf{h}}_i\}_{i=1}^N$  with updated coordinates  $\{\tilde{x}_i\}_{i=1}^N$ , which are passed to the RBA module.

Similarly, we stack  $L_e$  of SNE layers to learn the substrate atom representation  $\{\mathbf{z}_j\}_{j=1}^M$  from the embedding of the  $j$ -th substrate atom chemical feature  $\mathbf{z}_j^{(1)} = \text{Emb}(a_j)$ , but we do not update the atom coordinates.

### 3.4 Residue-atom Bi-scale Attention (RBA)

RBA aims to enhance pocket residues in both feature and coordinate spaces by jointly modeling (I) residue-residue and (II) residue-substrate interactions (Figure 2(b)).

**(I) Intra-Residue Attention.** To capture global message exchange within the enzyme, we perform the intra-residue attention to integrate intra-residue message using a radial basis function  $\phi_{\text{rbf}}$  based on the refined residue representations

$\{\tilde{\mathbf{h}}_i\}_{i=1}^N$  and coordinates  $\{\tilde{x}_i\}_{i=1}^N$ . Specifically, the attention weight  $\alpha_{ik}^r$  between the residue  $r_i$  and  $r_k$  is calculated as:

$$\alpha_{ik}^r = \text{softmax}\left(\frac{(\mathbf{q}_i^r)^\top \mathbf{k}_k^r}{\sqrt{d}} + \mathbf{W}_r^\top \phi_{\text{rbf}}(\|\tilde{x}_i - \tilde{x}_k\|_2)\right), \quad (9)$$

where  $\mathbf{q}_i^r = \mathbf{W}_Q^r \cdot \text{LN}(\tilde{\mathbf{h}}_i)$ ,  $\mathbf{k}_k^r = \mathbf{W}_K^r \cdot \text{LN}(\tilde{\mathbf{h}}_k)$ , and  $\mathbf{v}_k^r = \mathbf{W}_V^r \cdot \text{LN}(\tilde{\mathbf{h}}_k)$  are the query, key, and value projections of residue representation, and  $\mathbf{W}_{[\cdot]}$  is a linear projection weight.

The intra-residue message  $\mathbf{m}_i^r$  from neighboring residues and the coordinate update amount  $\Delta x_i^{rr}$  for residue  $r_i$  are then computed as:

$$\mathbf{m}_i^r = \sum_{k \in \mathcal{N}(i)} \alpha_{ik}^r \mathbf{v}_k^r, \quad (10)$$

$$g_{ik}^r = \text{GLU}(\mathbf{q}_i^r; \mathbf{k}_k^r; \phi_{\text{rbf}}(\|\tilde{x}_i - \tilde{x}_k\|_2)), \quad (11)$$

$$\Delta x_i^{rr} = \sum_{k \in \mathcal{N}(i)} \alpha_{ik}^r g_{ik}^r \cdot \frac{\tilde{x}_i - \tilde{x}_k}{\|\tilde{x}_i - \tilde{x}_k\|_2}. \quad (12)$$

Here  $g_{ik}^r$  is the learnable gate weight controlling the magnitude of coordinate update between residue  $r_i$  and  $r_k$ , computed by a Gated Linear Unit (GLU) [Dauphin *et al.*, 2017].

**(II) Residue-Atom Attention.** To model the interaction between residues and substrate atoms, we perform cross-modal attention between them. The attention weights  $\beta_{ij}^{rs}$  between the residue  $r_i$  and the substrate atom  $v_j$  are computed as:

$$\beta_{ij}^{rs} = \text{softmax}_i\left(\frac{(\mathbf{q}_i^r)^\top \mathbf{k}_j^s}{\sqrt{d}} + \mathbf{W}_s^\top \phi_{\text{rbf}}(\|\tilde{x}_i - y_j\|_2)\right), \quad (13)$$

where  $\mathbf{k}_j^s = \mathbf{W}_K^s \cdot \text{LN}(\mathbf{z}_j)$ ,  $\mathbf{v}_j^s = \mathbf{W}_V^s \cdot \text{LN}(\mathbf{z}_j)$ ,  $\text{softmax}_i$  means normalizing over residues.

We perform the  $\text{softmax}_j$  to the same attention score to obtain the attention weight  $\beta_{ij}^{sr}$  over atoms. The residue message  $\mathbf{m}_i^{rs}$  and substrate atom message  $\mathbf{m}_j^{sr}$  is then aggregated as:

$$\mathbf{m}_i^{rs} = \sum_{j \in \mathcal{N}(i)} \beta_{ij}^{rs} \mathbf{v}_j^s, \quad (14)$$

$$\mathbf{m}_j^{sr} = \sum_{i \in \mathcal{N}(j)} \beta_{ij}^{sr} \mathbf{v}_i^r. \quad (15)$$

**Feature and Coordinate Updates.** Next, we update the representations and coordinates of pocket residue and substrate atom based on the obtained messages and attention weights. For accurately modeling pocket-substrate interactions, we only update the residue of the pocket sites  $\tilde{\mathcal{P}} = \{i \mid \min_{v_j \in \mathcal{V}} \|\tilde{x}_i - y_j\|_2 < d\}$  and all atom of substrate. Specifically, we integrate intra-residue and residue-substrate messages to obtained the updated representations  $\mathbf{h}_i'$  and  $\mathbf{z}_i'$ :

$$\mathbf{h}_i' = \begin{cases} \mathbf{h}_i + \text{FFN}(\mathbf{m}_i^r; \mathbf{m}_i^{rs}), & i \in \overline{\mathcal{M}} \cap \tilde{\mathcal{P}}, \\ \mathbf{h}_i, & \text{otherwise}, \end{cases} \quad (16)$$

$$\mathbf{z}_i' = \mathbf{z}_i + \text{FFN}(\mathbf{m}_i^{sr}). \quad (17)$$

Here  $\overline{\mathcal{M}}$  is the non-functionally conserved sites.

Then, we use two GLUs to respectively compute the gate weight  $g_{ij}^{rs}$  and  $g_{ij}^{sr}$  of residues and atoms based on Equation 11

and  $\mathbf{q}_i^r, \mathbf{k}_j^s, \tilde{x}_i, y_j$ . The coordinate update amount  $\Delta x_i^{rs}$  for residue  $r_i$  and  $\Delta y_j^{rs}$  for atom  $v_j$  are computed as:

$$\Delta x_i^{rs} = \sum_{j \in \mathcal{N}(i)} \beta_{ij}^{rs} \cdot g_{ij}^{rs} \cdot \frac{y_j - \tilde{x}_i}{\|\tilde{x}_i - y_j\|_2}, \quad (18)$$

$$\Delta y_j^{sr} = \sum_{i \in \mathcal{N}(j)} \beta_{ij}^{sr} \cdot g_{ij}^{sr} \cdot \frac{\tilde{x}_i - y_j}{\|\tilde{x}_i - y_j\|_2}. \quad (19)$$

Finally, coordinates of residues and atoms is updated as  $\mathbf{h}'_i$  and  $\mathbf{z}'_i$ , respectively:

$$\tilde{x}'_i = \begin{cases} \tilde{x}_i + \Delta x_i^{rr} + \Delta x_i^{rs}, & i \in \overline{\mathcal{M}} \cap \tilde{\mathcal{P}}, \\ \tilde{x}_i, & \text{otherwise,} \end{cases} \quad (20)$$

$$y'_j = y_j + \Delta y_j^{sr}. \quad (21)$$

We stack  $L_p$  of RBA modules to obtain the final representation  $\hat{\mathbf{h}}_i$  and coordinates  $\hat{x}_i$  and  $\hat{y}_j$ , a prediction head are then employed to predict amino acid type:

$$\hat{s}_i = \text{softmax}(\mathbf{W}_{\text{aa}} \hat{\mathbf{h}}_i + \mathbf{b}_{\text{aa}}), \quad (22)$$

where  $\mathbf{W}_{\text{aa}} \in \mathbb{R}^{|\mathcal{A}| \times h_d}$  and  $\mathbf{b}_{\text{aa}} \in \mathbb{R}^{|\mathcal{A}|}$  are trainable parameters, and  $|\mathcal{A}| = 20$  denotes the amino acid vocabulary size.

### 3.5 Training Objective

EnzyPGM is trained jointly using sequence reconstruction and structural refinement. The training loss  $\mathcal{L}$  considers the joint optimization objective, including the enzyme sequence loss  $\mathcal{L}_s$ , pocket loss  $\mathcal{L}_{\text{ps}}$ , enzyme coordinates loss  $\mathcal{L}_c$ , pocket coordinates loss  $\mathcal{L}_{\text{pc}}$ , and substrate coordinates loss  $\mathcal{L}_{\text{sub}}$ :

$$\mathcal{L}_s = \frac{1}{|\mathcal{M}|} \sum_{i \in \mathcal{M}} l_{\text{CE}}(s_i^{\text{gt}}, \hat{s}_i), \quad (23)$$

$$\mathcal{L}_{\text{ps}} = \frac{1}{|\mathcal{P}|} \sum_{i \in \mathcal{P}} l_{\text{CE}}(s_i^{\text{gt}}, \hat{s}_i), \quad (24)$$

$$\mathcal{L}_c = \frac{1}{|\mathcal{M}|} \sum_{i \in \mathcal{M}} l_{\text{Huber}}(x_i^{\text{gt}}, \hat{x}_i), \quad (25)$$

$$\mathcal{L}_{\text{pc}} = \frac{1}{|\mathcal{P}|} \sum_{i \in \mathcal{P}} l_{\text{Huber}}(x_i^{\text{gt}}, \hat{x}_i), \quad (26)$$

$$\mathcal{L}_{\text{sub}} = \frac{1}{|\mathcal{M}|} \sum_j l_{\text{Huber}}(y_j^{\text{gt}}, \hat{y}_j). \quad (27)$$

Here  $\mathcal{P}$  is the ground-truth of pocket residue sites.  $s_i^{\text{gt}}$  denotes the ground-truth amino acid type,  $x_i^{\text{gt}}$  and  $y_j^{\text{gt}}$  are correspond to real 3D coordinates of residue  $r_i$  and substrate atom  $v_j$ .  $l_{\text{CE}}$  and  $l_{\text{Huber}}$  denote cross-entropy and Huber loss, respectively. Then we obtain the total loss:

$$\mathcal{L} = \lambda_s \mathcal{L}_s + \lambda_{\text{ps}} \mathcal{L}_{\text{ps}} + \lambda_c \mathcal{L}_c + \lambda_{\text{pc}} \mathcal{L}_{\text{pc}} + \lambda_{\text{sub}} \mathcal{L}_{\text{sub}}, \quad (28)$$

where  $\lambda_{[\cdot]}$  are hyperparameters for balancing these losses.

Table 1: Statistics of EnzyPock. Sample size indicates the number of enzyme-substrate pairs. The middle two rows are the number of third and fourth-level EC families.

Dataset	Training	Validation	Test
Sample Size	83,062	483	791
Third-Level Family	161	18	24
Fourth-Level Family	973	30	33
Average Seq. Length	324	314	322

Table 2: Quantitative results on EnzyPock. The best and second-best results are marked in **bold** and underlined, respectively.

Method	AAR $\uparrow$	Vina score $\downarrow$	pLDDT $\uparrow$	scRMSD $\downarrow$	scTM $\uparrow$
ESM3 (1.4B)	0.76	-3.46	<b>77.87</b>	<u>5.26</u>	0.89
RFdiffusion2+IF (84M)	0.56	-6.65	68.70	6.36	0.86
EnzyControl (21M)	0.49	<u>-6.90</u>	58.74	8.54	0.77
EnzyGen (714M)	0.64	-6.65	60.46	9.64	0.75
EnzyPGM (798M)	<b>0.77</b>	<b>-7.12</b>	<u>74.87</u>	<b>3.10</b>	<b>0.91</b>
w/o intra-residue attention	0.73	-7.08	73.63	4.54	0.88
w/o residue-atom attention	0.73	-7.13	72.48	4.55	0.87
w/o pocket & substrate loss	0.73	-7.13	74.43	3.54	0.89
Freezing RFF	0.70	-6.82	69.75	6.16	0.84

Table 3: Quantitative results on EnzyBench.

Method	AAR $\uparrow$	Vina score $\downarrow$	pLDDT $\uparrow$	scRMSD $\downarrow$	scTM $\uparrow$
ESM3 (1.4B)	0.64	-6.58	<b>71.64</b>	13.89	0.72
RFdiffusion2+IF (84M)	0.32	-7.15	61.91	11.81	0.72
EnzyControl (21M)	0.35	-7.18	60.64	10.88	0.71
EnzyGen (714M)	<b>0.88</b>	<b>-8.27</b>	<u>70.10</u>	<b>6.37</b>	<b>0.82</b>
EnzyPGM (798M)	<u>0.71</u>	<u>-8.17</u>	67.77	<u>10.48</u>	<u>0.72</u>

## 4 Experiments

### 4.1 EnzyPock: Dataset Curation

To construct a unified enzyme-pocket dataset that includes enzymes, substrates, EC numbers, and substrate-binding pockets, we employ a data collection and processing pipeline. First, we collect the protein-ligand pairs on PDBbind and CrossDocked. Next, enzymes in these samples are identified via PDB<sup>1</sup>-to-UniProt<sup>2</sup> ID mapping and EC number annotation from UniProt. We then perform MSA on these enzymes according to their fourth-level EC families using the Muscle5 tool [Edgar, 2022] to identify conserved sites for each family. In practice, we select residues present at the same position in more than 30% sequences as the conserved sites. Finally, we extract the substrate-binding pockets based on Equation 1.

In this process, we observe that many enzymes consist of multiple chains, and merging all chains for processing degrades the quality of homologous MSA analysis. Concatenating these chains leads to excessively long sequences and increases training cost. Therefore, we retain only the first EC-annotated chain for multi-chain proteins.

On the other hand, we adopt them according to the priority order of PDBBind and CrossDocked when records from different datasets conflict because PDBBind is validated by biological wet-lab experiments and CrossDocked is mainly composed of model predictions, which makes the former more reliable. To prevent data leakage, all 17,404 PDB entries in EnzyPock are clustered with a sequence identity threshold of

<sup>1</sup><https://www.rcsb.org/>

<sup>2</sup><https://www.uniprot.org/>

Table 4: Binding affinity (Vina score) and Foldability (pLDDT) comparison across 9 main EC-2 families on EnzyPock.

Binding affinity (Vina score ↓)										
EC Family	1.1	2.1	2.3	2.7	3.2	3.5	4.1	5.2	5.3	Avg.
ESM3 (1.4B)	-4.55	-0.60	<b>-0.00</b>	-2.04	-1.53	-5.67	-0.91	-3.71	-0.14	-3.52
RFdiffusion2+IF (84M)	<b>-5.62</b>	<b>-6.38</b>	-9.14	<b>-8.57</b>	<b>-7.27</b>	-6.47	-6.88	-6.79	-5.30	-7.01
EnzyControl (21M)	-4.74	-6.28	-8.57	-8.48	-6.59	-6.45	-6.96	<b>-7.10</b>	-5.88	-6.93
EnzyGen (714M)	-4.75	-6.12	-9.03	-8.44	-6.36	-5.96	-6.97	-6.80	<b>-6.06</b>	-6.66
<b>EnzyPGM (798M)</b>	-4.89	-6.21	<b>-9.37</b>	-8.39	-6.97	<b>-6.85</b>	<b>-7.15</b>	-6.98	-5.84	<b>-7.14</b>
Foldability (pLDDT ↑)										
EC Family	1.1	2.1	2.3	2.7	3.2	3.5	4.1	5.2	5.3	Avg.
ESM3 (1.4B)	<b>83.41</b>	<b>80.82</b>	<b>82.21</b>	<b>75.80</b>	74.84	<b>80.37</b>	<b>67.18</b>	78.89	84.58	<b>77.91</b>
RFdiffusion2+IF (84M)	77.15	77.90	70.07	73.15	43.66	71.84	56.38	73.07	81.63	68.56
EnzyControl (21M)	68.59	76.06	71.05	70.58	37.74	55.16	50.05	62.83	82.42	58.62
EnzyGen (714M)	63.31	75.78	53.34	70.47	45.00	58.73	50.65	63.08	76.60	60.33
<b>EnzyPGM (798M)</b>	79.96	76.27	75.68	71.34	<b>75.59</b>	79.25	49.68	<b>79.38</b>	<b>85.34</b>	74.89

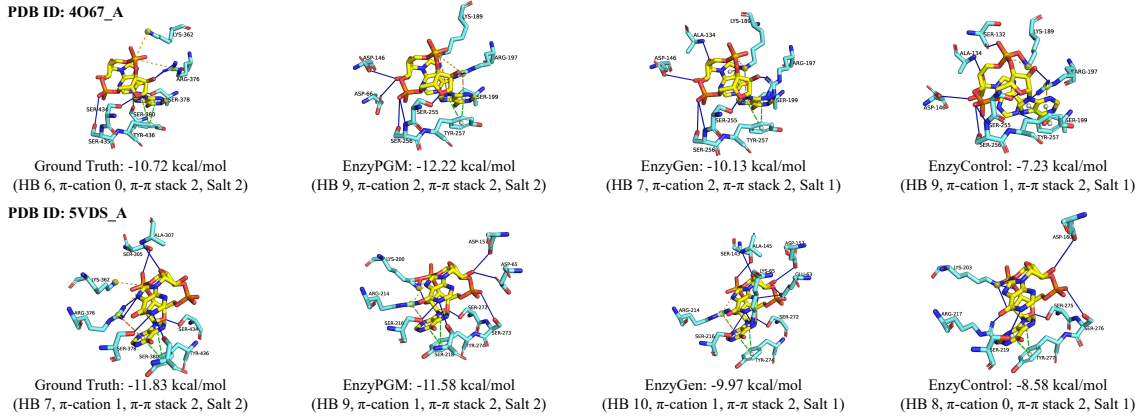


Figure 3: **Case Study.** Visualization of ground-truth, EnzyPGM-generated, and 2 baseline-generated enzyme-substrate complexes in order. Each panel displays the enzyme pocket (blue) and substrate (yellow), alongside key metrics: the Vina score (binding affinity) and the number of enzyme-substrate interactions: hydrogen bond (HB),  $\pi$ -cation,  $\pi$ - $\pi$  stack, and salt bridge (Salt).

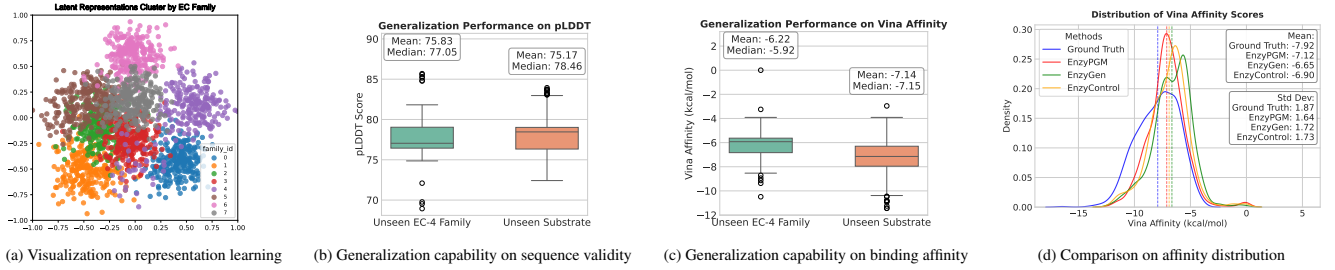


Figure 4: The different analysis on EnzyPGM.

70%. We split these samples of different clusters into training, validation, and test sets with non-overlapping clusters. The details of the dataset are shown in Table 1.

## 4.2 Experimental Settings

**Baselines:** (1) ESM3 [Hayes *et al.*, 2025] is an advanced multimodal protein language model generating the sequence, structure, and function of proteins; (2) RFdiffusion2+IF first uses RFdiffusion2 [Ahern *et al.*, 2025] to design enzyme structures based on given functionally important sites, then applies ProteinMPNN to generate sequences from the predicted structures; (3) EnzyControl [Song *et al.*, 2025] is a

diffusion model for enzyme backbone generation based on functional and substrate-specific control. (4) EnzyGen [Song *et al.*, 2024] is a substrate-specified enzyme generative model based on the given functionally conserved sites and EC label. Since ESM3 and RFdiffusion2 do not release their training script, we directly use their released model weight to generate the sequences. For EnzyControl, we use the public weight and follow their evaluation pipeline to test performance because we encounter challenges in using their code to train.

**Evaluation Metrics:** (1) Amino Acid Recovery (AAR) refers to the percentage of correctly recovered residue types in generated enzymes; (2) Vina score [Trott and Olson, 2010] to



evaluate the binding affinity between enzymes and substrates using Glna [McNutt *et al.*, 2021]; (3) pLDDT [Jumper *et al.*, 2021] to measure the foldability of generated sequences using ESMFold [Lin *et al.*, 2023]; (4) scRMSD [Trippe *et al.*, 2023] to assess the structural validity of generated backbones; (5) scTM to evaluate the structural design quality of generated enzymes. We adopt these metrics on EnzyPock and EnzyBench to test the performance of different approaches. To ensure a fair comparison between sequence- and structure-only modeling approaches, we uniformly use ESMFold-predicted structures to evaluate structure-related metrics, thereby eliminating evaluation variations from different modeling ways.

**Implementation Details:** EnzyPGM is composed of three stacked RFF and RBA modules, where each RFF contains 11 Transformer blocks initialized with ESM2 weights [Lin *et al.*, 2022]. A total of 3 individual SNE layers are used to process the substrate, and RBA only updates the pocket area within a 10Å radius of the substrate. The total parameter of EnzyPGM is 798M. The spatial  $K$ -nearest neighbor number in RFF, substrate SNE, and RBA are set to 30, 16, and 10, respectively. The hyperparameters  $\lambda_s$ ,  $\lambda_{ps}$ ,  $\lambda_c$ ,  $\lambda_{pc}$ , and  $\lambda_{sub}$  are set to 1, 0.5, 1, 0.5, and 1, respectively. For training EnzyPGM on EnzyPock, we adopt AdamW with a learning rate of 1e-5 and a cosine learning schedule, dynamic batch size on GPU memory capacity, and use four NVIDIA A100 GPUs to train 30 epochs with 8000 warmup steps.

### 4.3 Quantitative Results

**EnzyPGM realizes more effective enzyme design.** As shown in Table 2, EnzyPGM achieves the highest AAR of 0.77 and the lowest Vina score of -7.12 on EnzyPock, surpassing EnzyGen by 0.13, reducing the average binding energy by 0.47 kcal/mol. Meanwhile, EnzyPGM exhibits state-of-the-art performance in scRMSD and scTM on EnzyPock, suggesting the generated enzymes are well-folded and of high substrate affinity. Notably, ESM3 obtains the highest pLDDT on EnzyPock, showing that large-scale pre-training promotes the enzyme design learning, while EnzyPGM achieves a close level through fine-tuning. Also, we test all approaches on EnzyBench (Table 3), confirming that EnzyPGM has desirable performance and generalization, particularly in binding affinity. Specifically, we demonstrate the performance of all approaches on 9 main EC-2 families of EnzyPock in Table 4. These results demonstrate that pocket modeling benefits to generate enzymes with higher substrate-binding capability and structural validity, leading to more effective enzyme design.

### 4.4 Ablation Studies

**All designs in EnzyPGM contribute to enzyme generation.** We conduct ablation experiments to assess the contribution of core designs in EnzyPGM, which are the intra-residue and residue-atom attention, pocket and substrate loss, and RFF module. As shown in Table 2, removing two attentions results in a 1.24 and 2.39 drop in pLDDT, respectively. This confirms that the bi-scale attention improves performance in enzyme sequence design. Removing the pocket and substrate loss leads to a modest drop in overall performance, confirming that they promote model training. Freezing the RFF during training results in a performance drop across all metrics, suggesting

that the backbone model is essential for EnzyPGM. These results confirm that EnzyPGM’s core design jointly promote its enzyme design performance.

## 4.5 Case Studies

**EnzyPGM designs high-affinity binding pockets.** To demonstrate EnzyPGM’s performance in generating pockets, we perform a case study to compare it with 2 baselines and the ground truth. Visualization in Figure 3 reveals that EnzyPGM generates valid substrate-binding pockets with a lower Vina score than baselines and more abundant hydrogen bonds, which means the residues in the pocket form strong chemical bonds with the substrate. In contrast, EnzyGen and EnzyControl generate irregular binding regions where residues struggle to form stable chemical bonds with the substrate. These results highlight that pocket-conditioned training not only improves enzyme design quality but also generates valid and stable substrate-binding pockets.

## 5 Analysis

To gain deeper insights into EnzyPGM, we conduct comprehensive empirical analysis, including representation analysis, generalization evaluations, and binding affinity studies.

### 5.1 EnzyPGM learns EC family-aware representations

We project 2,000 enzymes into representation space from 8 EC-4 families by EnzyPGM and use t-SNE [Maaten and Hinton, 2008] to visualize their latent distribution. As shown in Figure 4(a), enzymes form distinct, well-separated clusters according to different families, which means that enzymes catalyzing similar reactions cluster naturally. This demonstrates that EnzyPGM learns function-aware latent representations, which benefits the design of substrate-specific enzymes.

### 5.2 EnzyPGM generalizes on unseen families and novel substrates

To evaluate generalization, we construct a test set that excludes all EC-4 families and substrates that appear in the training set. As shown in Figure 4(b) and 4(c), EnzyPGM achieves an average pLDDT of 75.83 and Vina score of -6.22 on unseen families, 75.17 and -7.14 on unseen substrates. The performance is almost consistent with the full test set, which indicates EnzyPGM can effectively design enzymes with high substrate binding for unseen reactions without retraining.

### 5.3 EnzyPGM designs enzymes with normal affinity distributions

We demonstrate the distribution of Vina scores obtained by different approaches in the EnzyPock test set. As shown in Figure 4 (d), the distribution obtained by EnzyPGM is closer to the ground truth than other approaches, with a closer mean and lowest variance. This demonstrates that EnzyPGM can design normal binding pockets for specific enzymatic reactions.

## 6 Conclusion

In this work, we have proposed EnzyPGM, a unified pocket-conditioned generative model for substrate-specific enzyme design. Unlike prior approaches, it integrates residue-atom bi-scale attention to model pocket-substrate interactions and fuse enzyme function priors to design enzymes with the binding pocket. To jointly model enzymes and pockets, we also curate EnzyPock, a comprehensive dataset with 84,336 enzyme-substrate pairs across 1,036 fourth-level EC families. Experiments on EnzyPock show EnzyPGM outperforms state-of-the-art methods in both binding affinity and structure validity metrics. Further analyses confirm its strong generalization to unseen families and novel substrates, highlighting its effectiveness for substrate-specific enzyme design.

## References

- [Ahern *et al.*, 2025] Woody Ahern, Jason Yim, Doug Tischer, Saman Salike, Seth M Woodbury, Donghyo Kim, Indrek Kalvet, Yakov Kipnis, Brian Coventry, Han Raut Altae-Tran, et al. Atom level enzyme active site scaffolding using rfdiffusion2. *bioRxiv*, page 2025.04.09.648075, 2025.
- [Baek *et al.*, 2021] Minkyung Baek, Frank DiMaio, Ivan Anishchenko, Justas Dauparas, Sergey Ovchinnikov, Gyu Rie Lee, Jue Wang, Qian Cong, Lisa N Kinch, R Dustin Schaeffer, et al. Accurate prediction of protein structures and interactions using a three-track neural network. *Science*, 373(6557):871–876, 2021.
- [Bar-Even *et al.*, 2011] Arren Bar-Even, Elad Noor, Yonatan Savir, Wolfram Liebermeister, Dan Davidi, {Dan S.} Tawfik, and Ron Milo. The moderately efficient enzyme: Evolutionary and physicochemical trends shaping enzyme parameters. *Biochemistry*, 50(21):4402–4410, May 2011.
- [Capra and Singh, 2007] John A Capra and Mona Singh. Predicting functionally important residues from sequence conservation. *Bioinformatics*, 23(15):1875–1882, 2007.
- [Chu *et al.*, 2024] Alexander E Chu, Tianyu Lu, and Po-Ssu Huang. Sparks of function by de novo protein design. *Nature Biotechnology*, 42(2):203–215, 2024.
- [Dauparas *et al.*, 2022] Justas Dauparas, Ivan Anishchenko, Nathaniel Bennett, Hua Bai, Robert J Ragotte, Lukas F Milles, Basile IM Wicky, Alexis Courbet, Rob J de Haas, Neville Bethel, et al. Robust deep learning-based protein sequence design using proteinmpnn. *Science*, 378(6615):49–56, 2022.
- [Dauparas *et al.*, 2025] Justas Dauparas, Gyu Rie Lee, Robert Pecoraro, Linna An, Ivan Anishchenko, Cameron Glasscock, and David Baker. Atomic context-conditioned protein sequence design using ligandmpnn. *Nature Methods*, pages 1–7, 2025.
- [Dauphin *et al.*, 2017] Yann N Dauphin, Angela Fan, Michael Auli, and David Grangier. Language modeling with gated convolutional networks. In *ICML*, pages 933–941. PMLR, 2017.
- [Du *et al.*, 2025] Jiahe Du, Kaixiong Zhou, Xinyu Hong, Zhaozhuo Xu, Jinbo Xu, and Xiao Huang. Retrieval augmented zero-shot enzyme generation for specified substrate. In *ICML*, 2025.
- [Edgar, 2022] Robert C Edgar. Muscle5: High-accuracy alignment ensembles enable unbiased assessments of sequence homology and phylogeny. *Nature communications*, 13(1):6968, 2022.
- [Ferruz *et al.*, 2022] Noelia Ferruz, Steffen Schmidt, and Birte Höcker. Protgpt2 is a deep unsupervised language model for protein design. *Nature Communications*, 13(1):4348, 2022.
- [Hayes *et al.*, 2025] Thomas Hayes, Roshan Rao, Halil Akin, Nicholas J Sofroniew, Deniz Oktay, Zeming Lin, Robert Verkuil, Vincent Q Tran, Jonathan Deaton, Marius Wiggert, et al. Simulating 500 million years of evolution with a language model. *Science*, 387(6736):850–858, 2025.
- [Hsu *et al.*, 2022] Chloe Hsu, Robert Verkuil, Jason Liu, Zeming Lin, Brian Hie, Tom Sercu, Adam Lerer, and Alexander Rives. Learning inverse folding from millions of predicted structures. In *ICML*, pages 8946–8970. PMLR, 2022.
- [Hua *et al.*, 2024] Chenqing Hua, Jiarui Lu, Yong Liu, Odín Zhang, Jian Tang, Rex Ying, Wengong Jin, Guy Wolf, Doina Precup, and Shuangjia Zheng. Reaction-conditioned de novo enzyme design with genzyme. *arXiv preprint arXiv:2411.16694*, 2024.
- [Huang *et al.*, 2021] Juan Huang, Qin Xu, Zhuo Liu, Nitin Jain, Madhusudan Tyagi, Dong-Qing Wei, and Liang Hong. Controlling the substrate specificity of an enzyme through structural flexibility by varying the salt-bridge density. *Molecules*, 26(18):5693, 2021.
- [Jumper *et al.*, 2021] John Jumper, Richard Evans, Alexander Pritzel, Tim Green, Michael Figurnov, Olaf Ronneberger, Kathryn Tunyasuvunakool, Russ Bates, Augustin Žídek, Anna Potapenko, et al. Highly accurate protein structure prediction with alphafold. *Nature*, 596(7873):583–589, 2021.
- [Kortemme, 2024] Tanja Kortemme. De novo protein design—from new structures to programmable functions. *Cell*, 187(3):526–544, 2024.
- [Lesk, 2001] Arthur M Lesk. *Introduction to protein architecture: the structural biology of proteins*, volume 741. Oxford university press Oxford, 2001.
- [Lin *et al.*, 2022] Zeming Lin, Halil Akin, Roshan Rao, Brian Hie, Zhongkai Zhu, Wenting Lu, Allan dos Santos Costa, Maryam Fazel-Zarandi, Tom Sercu, Sal Candido, et al. Language models of protein sequences at the scale of evolution enable accurate structure prediction. *bioRxiv*, 2022.
- [Lin *et al.*, 2023] Zeming Lin, Halil Akin, Roshan Rao, Brian Hie, Zhongkai Zhu, Wenting Lu, Nikita Smetanin, Robert Verkuil, Ori Kabeli, Yaniv Shmueli, et al. Evolutionary-scale prediction of atomic-level protein structure with a language model. *Science*, 379(6637):1123–1130, 2023.
- [Maaten and Hinton, 2008] Laurens van der Maaten and Geoffrey Hinton. Visualizing data using t-sne. *JMLR*, 9(Nov):2579–2605, 2008.



- [McNutt *et al.*, 2021] Andrew T. McNutt, Paul Francoeur, Rishal Aggarwal, Tomohide Masuda, Rocco Meli, Matthew Ragoza, Jocelyn Sunseri, and David Ryan Koes. GNINA 1.0: Molecular docking with deep learning. *Journal of Cheminformatics*, 13(1):43, June 2021.
- [Meshchaninov *et al.*, 2025] Viacheslav Meshchaninov, Pavel Strashnov, Andrey Shevtsov, Fedor Nikolaev, Nikita Ivanisenko, Olga Kardymon, and Dmitry Vetrov. Diffusion on language model encodings for protein sequence generation. In *ICML*, 2025.
- [Nijkamp *et al.*, 2023] Erik Nijkamp, Jeffrey A Ruffolo, Eli N Weinstein, Nikhil Naik, and Ali Madani. Progen2: exploring the boundaries of protein language models. *Cell Systems*, 14(11):968–978, 2023.
- [Notin *et al.*, 2024] Pascal Notin, Nathan Rollins, Yarin Gal, Chris Sander, and Debora Marks. Machine learning for functional protein design. *Nature Biotechnology*, 42(2):216–228, 2024.
- [Satorras *et al.*, 2021] Victor Garcia Satorras, Emiel Hoogeboom, and Max Welling. E (n) equivariant graph neural networks. In *ICML*, pages 9323–9332. PMLR, 2021.
- [Song *et al.*, 2024] Zhenqiao Song, Yunlong Zhao, Wenxian Shi, Wengong Jin, Yang Yang, and Lei Li. Generative enzyme design guided by functionally important sites and small-molecule substrates. In *ICML*, pages 46259–46279. PMLR, 2024.
- [Song *et al.*, 2025] Chao Song, Zhiyuan Liu, Han Huang, Liang Wang, Qiong Wang, Jian-Yu Shi, Hui Yu, Yihang Zhou, and Yang Zhang. Enzycontrol: Adding functional and substrate-specific control for enzyme backbone generation. In *NeurIPS*, 2025.
- [Stank *et al.*, 2016] Antonia Stank, Daria B Kokh, Jonathan C Fuller, and Rebecca C Wade. Protein binding pocket dynamics. *Accounts of Chemical Research*, 49(5):809–815, 2016.
- [Stärk *et al.*, 2022] Hannes Stärk, Octavian Ganea, Lagnajit Pattanaik, Regina Barzilay, and Tommi Jaakkola. Equibind: Geometric deep learning for drug binding structure prediction. In *ICML*, pages 20503–20521. PMLR, 2022.
- [Tipton and Boyce, 2000] Keith Tipton and Sinéad Boyce. History of the enzyme nomenclature system. *Bioinformatics*, 16(1):34–40, 2000.
- [Trippe *et al.*, 2023] Brian L Trippe, Jason Yim, Doug Tischer, David Baker, Tamara Broderick, Regina Barzilay, and Tommi S Jaakkola. Diffusion probabilistic modeling of protein backbones in 3d for the motif-scaffolding problem. In *ICLR*, 2023.
- [Trott and Olson, 2010] Oleg Trott and Arthur J Olson. Autodock vina: improving the speed and accuracy of docking with a new scoring function, efficient optimization, and multithreading. *Journal of Computational Chemistry*, 31(2):455–461, 2010.
- [Vaswani *et al.*, 2017] Ashish Vaswani, Noam Shazeer, Niki Parmar, Jakob Uszkoreit, Llion Jones, Aidan N Gomez, Łukasz Kaiser, and Illia Polosukhin. Attention is all you need. *NeurIPS*, 30, 2017.
- [Wang *et al.*, 2024] Xinyou Wang, Zaixiang Zheng, Fei Ye, Dongyu Xue, Shujian Huang, and Quanquan Gu. Diffusion language models are versatile protein learners. In *ICML*, pages 52309–52333. PMLR, 2024.
- [Wang *et al.*, 2025] Yuhang Wang, Shuangxin Han, Yi Wang, Quanfeng Liang, and Wei Luo. Artificial intelligence technology assists enzyme prediction and rational design. *Journal of Agricultural and Food Chemistry*, 73(12):7065–7073, 2025.
- [Watson *et al.*, 2023] Joseph L Watson, David Juergens, Nathaniel R Bennett, Brian L Trippe, Jason Yim, Helen E Eisenach, Woody Ahern, Andrew J Borst, Robert J Ragotte, Lukas F Milles, et al. De novo design of protein structure and function with rfdiffusion. *Nature*, 620(7976):1089–1100, 2023.
- [Xiong *et al.*, 2020] Ruibin Xiong, Yiming Yang, Di He, Kai Zheng, Shuxin Zheng, Chenxiang Xing, Huishuai Zhang, Yanyan Lan, Liqiang Wang, and Tie-Yan Liu. On layer normalization in the transformer architecture. *arXiv preprint arXiv:2002.04745*, 2020.
- [Zhang *et al.*, 2024a] Zaixi Zhang, Wan Xiang Shen, Qi Liu, and Marinka Zitnik. Efficient generation of protein pockets with pocketgen. *Nature Machine Intelligence*, 6(11):1382–1395, 2024.
- [Zhang *et al.*, 2024b] Zaixi Zhang, Marinka Zitnik, and Qi Liu. Generalized protein pocket generation with prior-informed flow matching. *NeurIPS*, 37:38559–38589, 2024.